

# Can the liver Regenerative Potential Restore the Normal Liver Structure in Male Mice CCL4 Induced Liver Fibrosis? A Histological and Immunohistochemical Study

Original  
Article

Heba M. Saad Eldien<sup>1,2</sup>, Nashwa A. M. Mostafa<sup>2</sup> and Randa Abd El Aziz Mohamed<sup>2</sup>

<sup>1</sup>Anatomy Department, College of Medicine, Jouf University, KSA.

<sup>2</sup>Histology and Cell Biology Department, Faculty of Medicine, Assiut university, Egypt

## ABSTRACT

**Background:** Liver fibrosis is a major Egyptian health problem and a serious threat to human health. It is characterized by repeated injury of the liver tissue resulting in the excessive accumulation of extracellular matrix. Liver is the only visceral organ that possesses unique capacity to regenerate.

**Aim of Work:** To investigate the role of the regenerative capacity of the liver in restoring the normal structure after withdrawal of carbon tetrachloride (CCL4) in mice.

**Materials and Methods:** A total number of thirty male healthy mice was used in the present study. The animals were randomly divided into three groups (10 mice each): Group I: (control group = GI). Group II: (CCL4 alone group = GII) were injected 1 ml/kg carbon tetrachloride (CCL4) dissolved in olive oil (1:1) twice a week for 4 weeks intraperitoneally. At the end of 4 weeks they were sacrificed. Group III (CCL4/recovery group = GIII): were injected with CCL4 as previous group, then left for another four weeks without any intervention before sacrifice. At the end of the experiment, the liver was immediately dissected out and processed for histological and immunohistochemical examinations.

**Results:** In GII, there was marked disturbance of liver architecture in the form of marked cellular infiltration and vacuolation associated with significant increase in the collagen and reticular fibers as well as increased expression of anti  $\alpha$ -smooth muscle actin in hepatic stellate cells. Proliferative cells were observed in excess as indicated by increase in immunofluorescent staining of anti KI67. In GIII, moderate improvement was observed in liver architecture. Significant reduction in ALT and AST was also observed. On the other hand, serum albumin level was significantly increased compared to (GII).

**Conclusion:** Withdrawal of CCL4 produced moderate improvement in the structure of the liver. As CCL4 chronic exposure exceeds the regenerative capacity of the liver to restore the normal structure.

**Received:** 21 May 2019, **Accepted:** 17 July 2019

**Key Words:**  $\alpha$ -smooth muscle, CCL4, liver, regeneration.

**Corresponding Author:** Nashwa A. M. Mostafa, PhD, Histology and Cell Biology, Faculty of Medicine, Assiut, Egypt, Tel.: +20 1002866348, E-mail: nashwa20012002us@yahoo.com

ISSN: 1110-0559, Vol. 43, No. 1

## INTRODUCTION

The liver is a unique organ; it performs several important functions such as detoxification, metabolic activities and immunity<sup>[1]</sup>.

One of the serious Egyptian health problems is liver fibrosis<sup>[2]</sup>. It is associated with increase in the formation of extracellular matrix that results in many complications<sup>[3]</sup>, such as ascites, variceal hemorrhage, and encephalopathy<sup>[2]</sup>. Liver fibrosis is a result of many liver diseases as hepatitis B and C (HBV and HCV) viral infection, malignant liver tumors, and Wilson's disease<sup>[4]</sup>.

Liver fibrosis is induced in experimental animals by Carbon tetrachloride (CCl4) that produces disturbance in liver structure similar to human chronic diseases<sup>[5]</sup>.

Cells (HSCs). It can be activated and changed into myofibroblasts when the liver is damaged. Myofibroblasts are positive for alpha smooth muscle actin ( $\alpha$ -SMA)

and they produce excessive collagen that results in liver fibrosis<sup>[6,7]</sup>.

Liver is a unique visceral organ that is characterized by the ability to regenerate. Hepatocytes change from being quiescent, they can quickly be activated and divided to restore normal liver structure<sup>[8]</sup>. Few studies have dealt with investigating the regenerative potential of the liver in mice with liver fibrosis induced by CCL4 as regards the hepatic stellate cells. We therefore aimed to investigate this potential, after withdrawal of CCL4, on the liver architecture.

## MATERIALS AND METHODS

After approval of the institutional Committee of Ethics in Assiut University, thirty male BALB/C healthy mice (40 gm body weight each) were used in this study. They were housed in clean capacious cages under strict care, hygiene and appropriate temperature at the animal house

of the faculty of Medicine, Assiut University. They were fed standard diet and water.

Animals were divided randomly into the following three groups (n=10): Group I: (control group = GI) mice in this group divided into two subgroups: subgroup IA, as a negative control (5 mice), they were left without intervention. Subgroup IB, as a positive control (5 mice), each animal was given 0.5 ml of olive oil (vehicle for CCL4) twice a week for four weeks intraperitoneally. Group II: (CCL4 group) mice were injected with CCL4 intraperitoneally<sup>[9]</sup> with 1 ml/kg carbon tetrachloride (CCL4) (El Nasr Pharmaceutical and Chemical Company (Cairo, Egypt), dissolved in olive oil (1:1) twice a week for 4 weeks. Group III: (CCL4/recovery group): mice were injected with CCL4 as the previous group, then left for another four weeks without any intervention before sacrifice. Mice were sacrificed after ether inhalational anesthesia. Blood was taken from retro-orbital vein and used to measure liver enzymes and albumin. The liver specimens were taken and prepared for light microscopy. Paraffin sections of 5  $\mu$ m thickness were obtained and subjected to the following techniques: Histological criteria were studied using Hematoxylin and Eosin stain. Collagen fibers assessment was done using Masson trichrome stain and reticular fibers by silver stain<sup>[10]</sup>. Immuno-histochemical staining for: Alpha smooth muscle actin antigen using anti - ( $\alpha$  SMA) antibody (for detection of activated HSCs<sup>[11,12]</sup>. Immuno-fluorescence staining for KI 67 using anti-KI67 antibody: for detection of proliferating cells.

#### ***For Immuno-Histochemical Staining***

Sections were deparaffinized, rehydrated in descending grades of ethyl alcohol down then distilled water. Boiling of the tissue sections was done in 10 ml citrate buffer in a microwave for 10 min for antigen retrieval. Then the sections were left to cool for 20 minutes. The primary antibody for  $\alpha$  SMA (NB P1-30894, rabbit monoclonal antibody, Novus-USA) was applied to the sections in dilution of 1:100. Then, the sections were incubated with secondary antibody (Biotinylated Goat Anti-polyvalent) for 30 minutes at room temperature. Incubation with "Streptavidin-Horseradish peroxidase" was done for 15 minutes at room temperature (Ultra Vision Detection System Anti-Polyvalent, HRP/DAB kit, Thermo Scientific, USA, catalogue number TP-015-HA). Slides were washed with distilled water after incubated at room temperature for 15 minutes with diaminobenzidine (DAB) chromogen. Counterstaining of slides was done with Meyer's hematoxylin. Dehydration, clearing, mounted and examined by light microscopy. Positive and negative controls were used. Control muscle was used as positive control. For negative control staining, some sections were incubated with PBS instead of the primary antibody. No immunoreactivity was present in these sections.

#### ***For Immunofluorescence Staining***

Staining was performed as previously described<sup>[13]</sup>, using rabbit polyclonal antibodies (Ki 67, ab15580,

Abcam, UK), 1:200, dilution was used followed by incubation with Alexa Fluor 647 conjugated secondary antibody in 1:500 dilution in blocking buffer for 2 h at room temperature (Alexa Fluor 647, Abcam,UK). Stained sections were mounted with fluorescent mounting medium. The reaction is nuclear for KI67. Thymus was used as positive control for KI67 staining. An isotope control was performed using rabbit-IgG with omission of the primary antibody. The fluorescent images were captured using a fluorescence microscope (Olympus microscope BX51) in Histology Department, faculty of Medicine, Assiut university.

#### ***Biochemical Study***

Blood samples were collected from the retro-orbital venous plexus of all groups under mild anaesthesia, using a fine heparinized capillary tube introduced into the medical epicanthus of the mouse eye<sup>[14]</sup>. The serum levels of Aspartate aminotransferase (AST), Alanine aminotransferase (ALT) and Serum albumin were assayed by the method of Reitman and Frankel<sup>[15]</sup>, using the commercial diagnostic kits.

#### ***Morphometric Study***

Morphometric measurements<sup>[16]</sup>, were carried out using a computerized image analyzer system software (Leica Q 500 MCO; Leica, Wetzlar, Germany) connected to a camera attached to a Leica universal microscope at the Histology Department, Faculty of Medicine, Assiut University. The following measures were done:

The mean area percentage of collagen fibers and reticular fibers,  $\alpha$  SMA positive cells, KI67 positive cells in the liver in Masson trichrome and silver stained sections,  $\alpha$  SMA and KI67 immune stained respectively was measured. The measurements were performed in 10 non-overlapping fields at magnification of x40 and one to two sections were taken from five different animals in each group.

#### ***Statistical Analysis***

Data were expressed as mean and standard error (SE) for the quantitative variable. Data were statistically analyzed using statistical package SPSS version 22. Comparisons between groups were done using ANOVA (analysis of variance) followed by Tukey's test for multiple comparisons between groups. Significance was set at a P value of less than 0.05 for all comparisons<sup>[17]</sup>.

## **RESULTS**

---

### ***I-Histological results***

#### ***1- Control group (GI)***

Histological examination of the liver in subgroup IA and IB showed nearly the same structures.

Examination of H&E stained liver sections of control mice showed that, the liver cells were radiated from the central vein in the form of cords toward the periphery of the lobules. They were separated from each other

by irregular vascular spaces, hepatic sinusoids. The Hepatocyte appeared with acidophilic cytoplasm and large central vesicular nucleus with prominent nucleolus. Some hepatocytes contain two nuclei (Figure1). At the periphery of hepatic lobule portal tracts were present, each tract contained branches of portal vein, hepatic artery and bile duct (Figure 2). With Masson trichrome stain, scanty fine collagen fibers were observed around the central vein. No collagen fibers were observed between the hepatocytes (Figure 3). With Silver stain, few brown reticular fibers were observed in the wall of central vein and between the liver cells (Figure 4)

## 2- CCL4 Treated Group (GII)

In H&E stain, the liver revealed disturbed architecture. Most of the hepatocytes had vacuolated cytoplasm. Many nuclei showed karyorrhexis, while other cells appeared with illdefined nuclei (Figure 5). Dilated central vein with intense cellular infiltration around it. Many hepatocytes appeared with dense nuclei and deeply acidophilic cytoplasm. Kupffer cells engulfing brown pigment were observed (Figure 6). Portal tract appeared not affected (Figure 7).

With Masson trichrome stain, increase in the collagen fibers was noticed around central vein and in between liver cells (Figure 8). With Silver stain, there was increase in the reticular fibers in the wall of central vein and in between the liver cells. It appeared as short thick brown to black fibers (Figure 9).

## 3- Recovery group (GIII)

Withdrawal of CCL4 for one month led to a moderate improvement in liver structure. There was a decrease in the cellular infiltration around the central vein. The hepatocytes had either vacuolated cytoplasm or deeply acidophilic cytoplasm and dense nuclei (Figure 10).

With Masson trichrome stain, thick collagen fibers was noticed around the central vein and in between liver cells (Figure 11). With Silver stain, numerous reticular fibers were observed, but they were finer than group II, in the wall of central vein and between the liver cells (Figure 12).

## Immunohistochemistry Results

Immunostaining of  $\alpha$ -SMA: In group I, positive dark brown immunoreaction to anti  $\alpha$ -SMA was seen in the media of central veins. No positive reaction was detected between the liver cells (Figure 13). In group II, there was a highly positive peri-sinusoidal reaction (Figure 14). In group III, there was a decrease in the positive peri-sinusoidal reaction compared to group II (Figure 15).

## Immunofluorescence Results for KI67

In group I, few positive nuclei of hepatocytes were observed (Figure 16). In group II, many positive nuclei were observed in the hepatocytes (Figure 17). In group III, few positive nuclei were detected but more than group I (Figure 18).

## II-Biochemical results

Serum ALT and AST showed a significant high level in CCL4 treated group. The recovery group showed significant level reduction (Table 1,2; Histogram 1,2).

There was a significant reduction of serum albumin of rats in CCL4 and recovery groups as compared to the control group. (Table 3, Histogram 3).

## III-Morphometric results

The area percentage of collagen fibers was significantly higher in GII compared with other groups (Table 4, Histogram 4). The area percentage of reticular fibers was significantly higher in GII compared with other groups (Table 5, Histogram 5). The area percentage of  $\alpha$ -SMA-positive cells was significantly higher in GII compared with other groups (Table 6, Histogram 6). The number of KI67-positive cells was significantly high in GII compared with other groups (Table 7, Histogram 7).

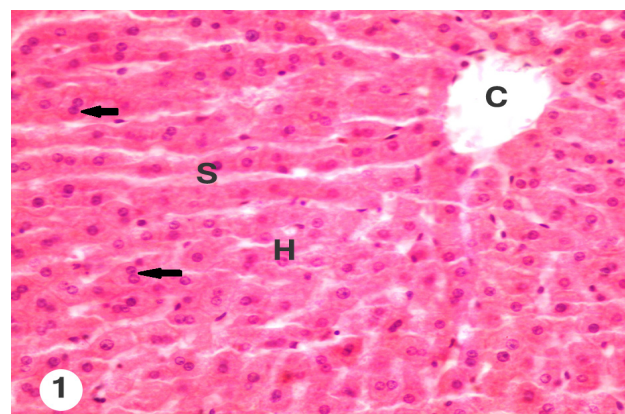


**Fig.1:** A photomicrograph of a section of the liver of G1 male mouse showing hepatic cords radiating from the central vein (C) and separated from each other by hepatic sinusoids (S). Note hepatocytes (H) with vesicular nuclei. Some hepatocytes contain two nuclei (arrow). H&E,  $\times$  400

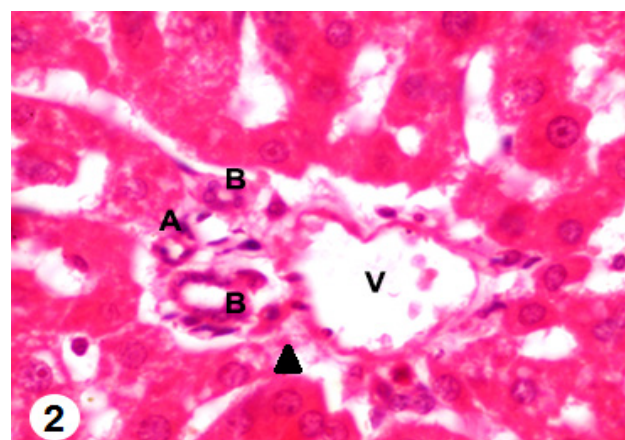


**Fig.2:** A photomicrograph of a section of the liver of G1 male mouse showing a portal tract with branches of hepatic artery (A), portal vein (V) and bile duct (B) surrounded by connective tissue (arrow head). H&E  $\times$  1000

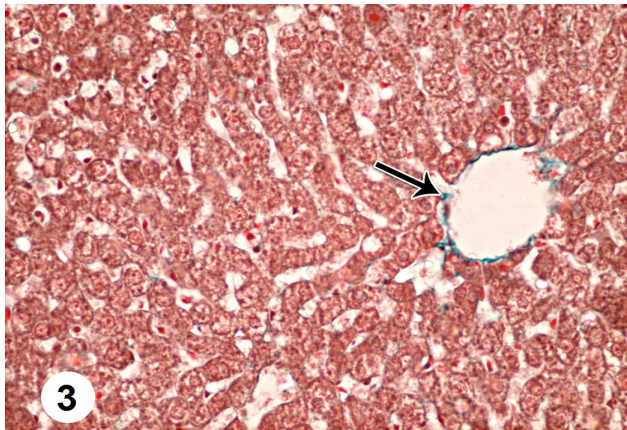


**Fig.3:** A photomicrograph of a section of the liver of G1 male mouse showing the scanty fine collagen fibers (arrow) around central vein. Notice: No collagen fibers are observed between the hepatocytes. Masson trichrome x400.

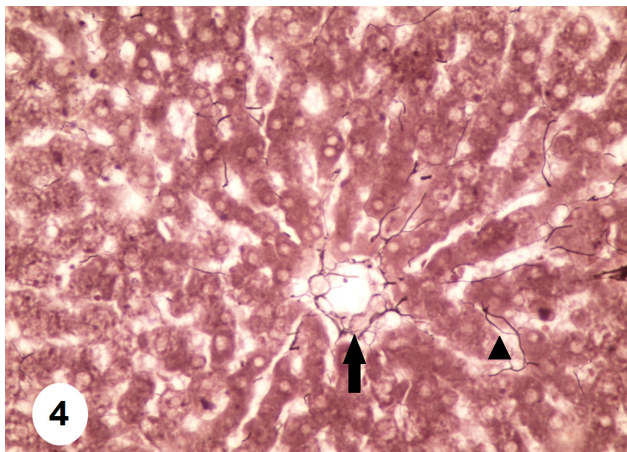


**Fig.4:** A photomicrograph of a section of the liver of G1 male mouse showing few brown reticular fibers are observed in the wall of central vein (arrow) and between the liver cells (arrowhead). Silver stain x400

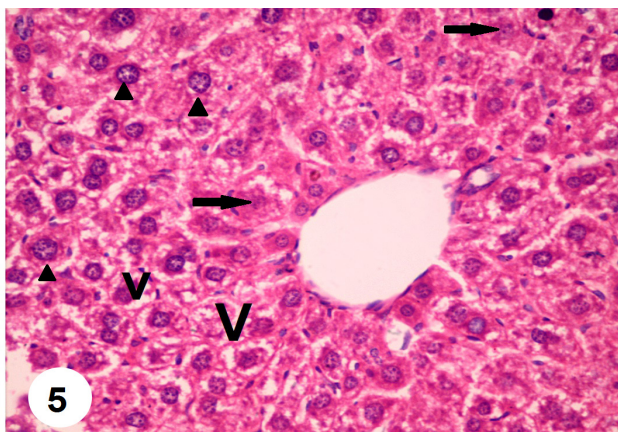


**Fig.5:** A photomicrograph of a section of the liver of group II male mouse, showing that most of the hepatocytes have vacuolated cytoplasm (v). Many nuclei show karyorrhexis (arrowhead). Other cells appear with illdefined nuclei (arrow). H&E × 400.

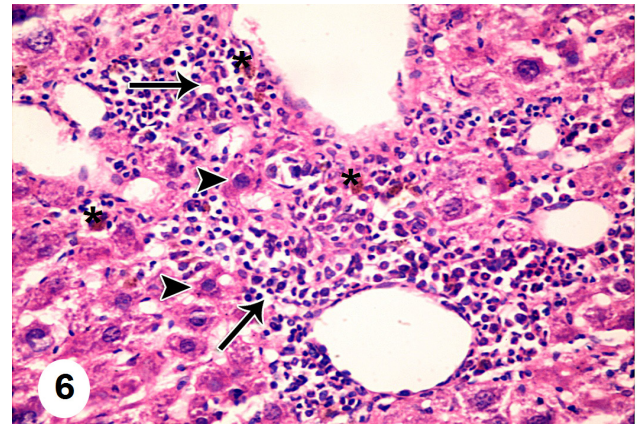


**Fig.6:** A photomicrograph of a section of the liver of group II male mouse, showing cellular infiltration (arrows) around the central vein. Notice many cells appear with deeply acidophilic cytoplasm and dense nuclei (arrow head). Also, Kupffer cells engulfing brownish pigment are observed (\*). H&E × 400.

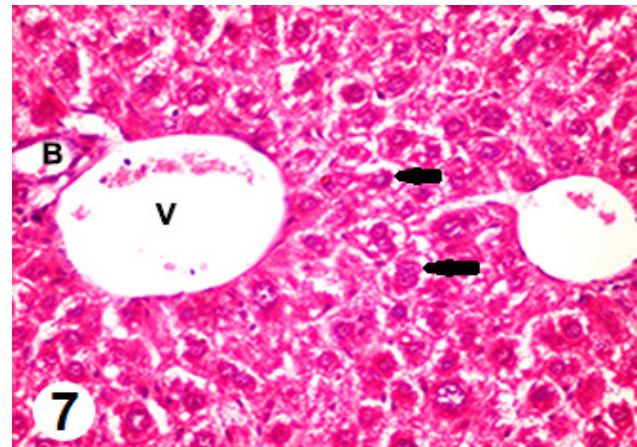


**Fig.7:** A photomicrograph of a section of the liver of group II male mouse, showing that the portal tract appear not affected. Notice, portal vein (v), bile duct (B). Also, many vacuolated cells are observed (arrow). H&E x 400

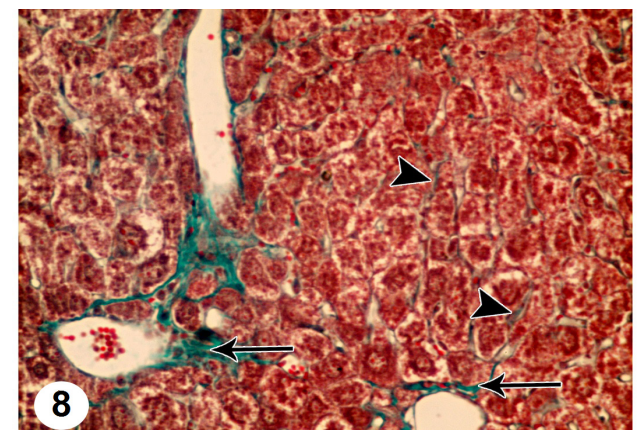


**Fig.8:** A photomicrograph of a section of the liver of group II male mouse, showing increase in collagen fibers deposition (arrows) around central vein and between the hepatic cells (arrowhead). Masson trichrome x400

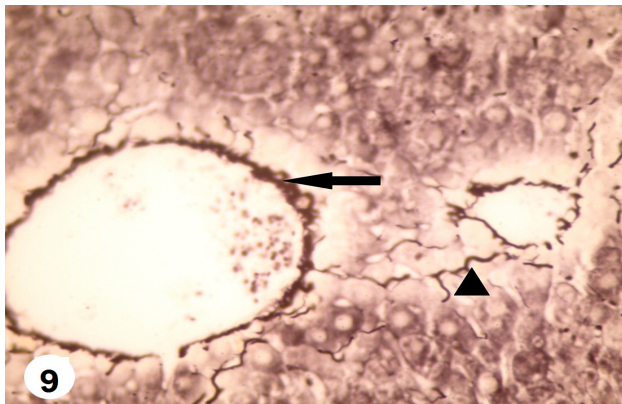


**Fig.9:** A photomicrograph of a section of the liver of group II male mouse, showing increase in the reticular fibers in the wall of central vein (arrow) and in between the liver cells. It appears as short thick fibers (arrowhead). Silver stain x 400

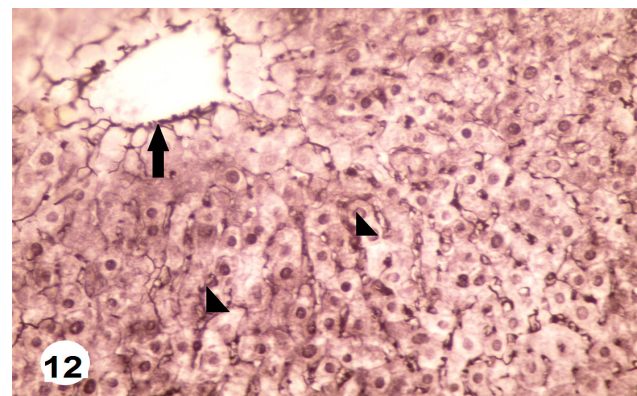


**Fig.12:** A photomicrograph of a section of the liver of group III male mouse, showing numerous reticular fibers, they are finer than group II. It appears in the wall of central vein (arrow) and between the liver cells (arrowhead). Silver stain x400

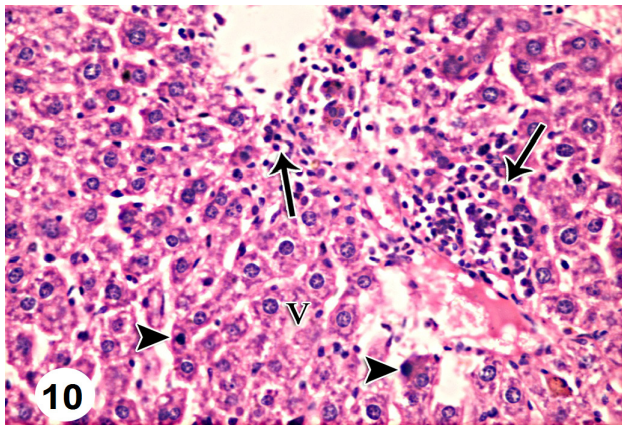


**Fig.10:** A photomicrograph of a section of the liver of group III male mouse, showing decrease the cellular infiltration around the central vein (arrow). Some hepatocytes have vacuolated cytoplasm (V). Notice: some cells with deeply acidophilic cytoplasm and dense nuclei (arrowhead). H&Ex400

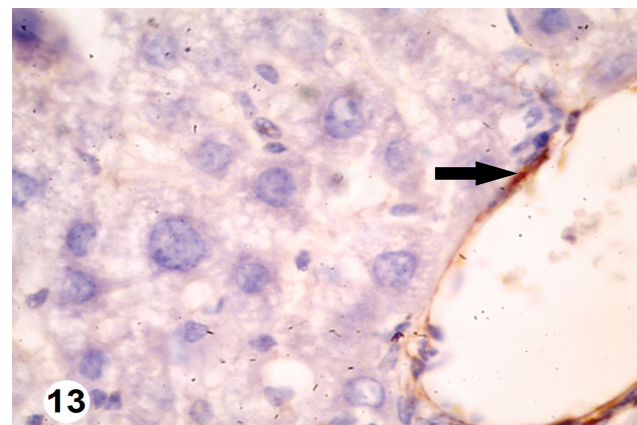


**Fig.13:** A photomicrograph of a section of the liver of group I male mouse, showing that positive dark brown immunoreaction is seen in the media of the central vein (arrow).No positive reaction is detected between the liver cells. Anti-  $\alpha$ -SMA immunostainingx1000

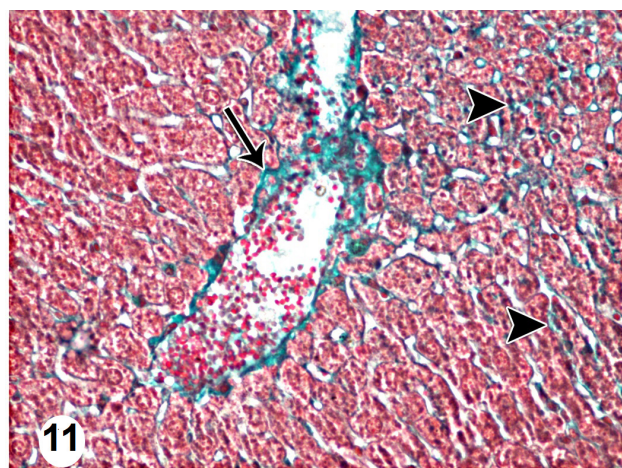


**Fig.11:** A photomicrograph of a section of the liver of group III male mouse, showing thick collagen fibers deposition around the central vein (arrow) and in between the liver cells (arrowhead). Massson trichrome x400.

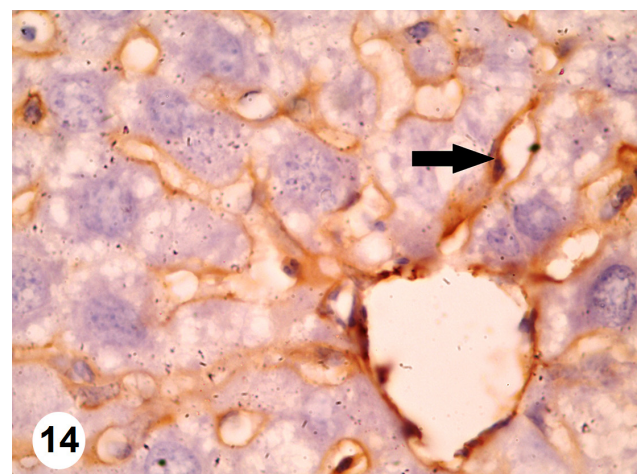


**Fig.14:** A photomicrograph of a section of the liver of group II male mouse, showing a highly positive reaction peri-sinusoidal (arrow). Anti-  $\alpha$ -SMA immunostainingx1000

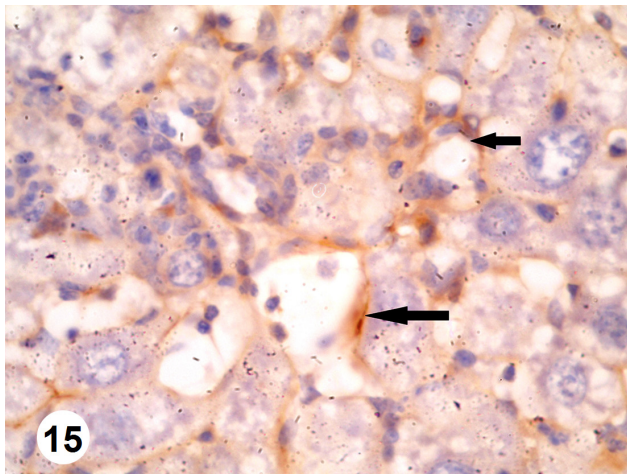


**Fig.15:** A photomicrograph of a section of the liver of group III male mouse, showing decrease in the positive reaction perisinusoidal (arrow). Anti- $\alpha$ -SMA immunostaining x1000

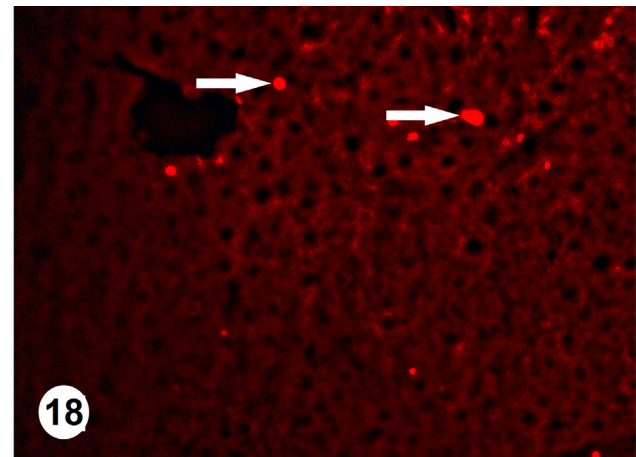


**Fig.18:** A photomicrograph of a section of the liver of group III male mouse, showing relatively few positive nuclei of hepatocytes in comparison to group I (arrow). Anti-KI67 immunofluorescence x400

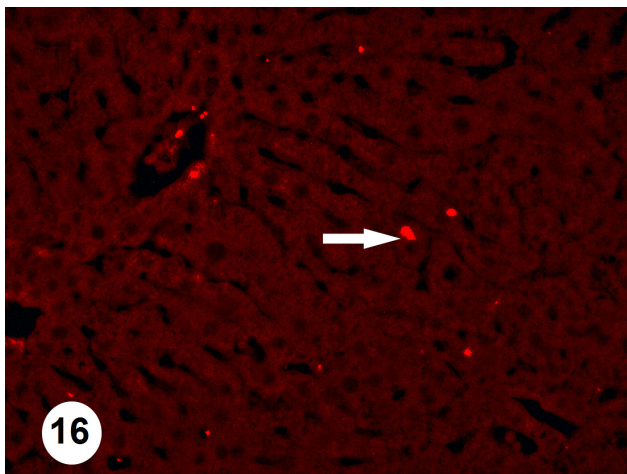


**Fig.16:** A photomicrograph of a section of the liver of group I male mouse, showing few scattered positive nuclei (arrow). Anti-KI 67 immunofluorescence x400

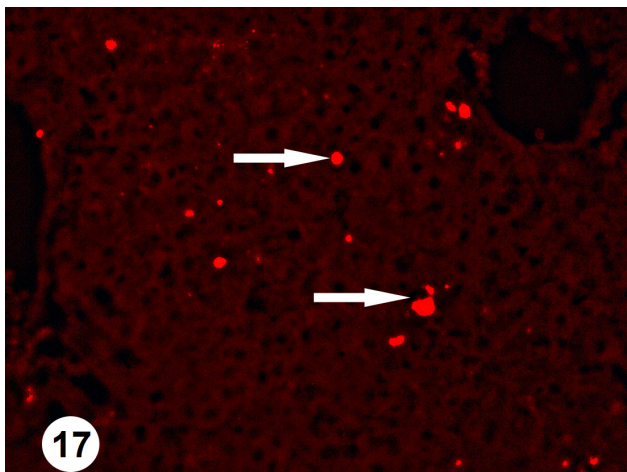
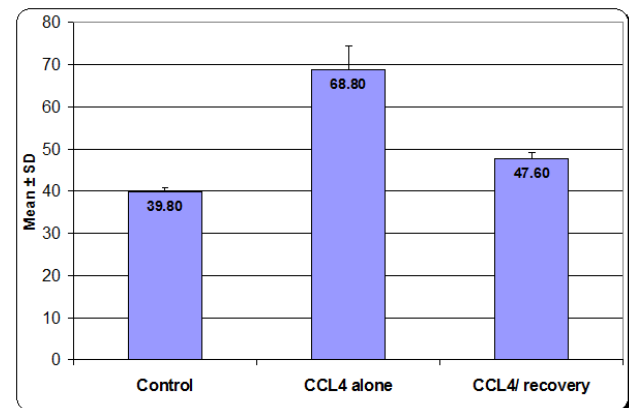


**Fig.17:** A photomicrograph of a section of the liver of group II male mouse, showing multiple scattered positive nuclei are observed in the hepatocytes (arrow). Anti-KI67 immunofluorescence x400

**Table 1:** Mean values ( $\pm$ SE) of ALT level in the studied groups (U/L)

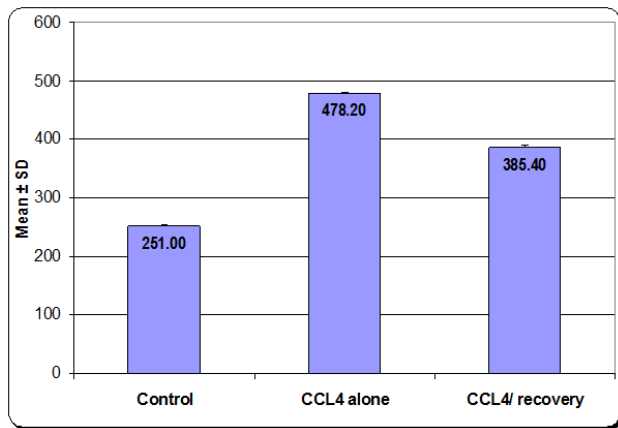
ALT (U/L)	Control	CCL4 alone	CCL4/ recovery
Mean $\pm$ SD	39.80 $\pm$ 0.84	68.80 $\pm$ 5.40	47.60 $\pm$ 1.67
Range	39.0 - 41.0	63.0 - 77.0	45.0 - 49.0
<i>P-value</i> <sup>1</sup>		0.009*	0.008*
<i>P-value</i> <sup>2</sup>			0.009*



**Histogram 1:** comparing the mean values of ALT level in the studied groups.

**Table 2:** Mean values ( $\pm$ SE) of AST level in the studied groups (U/L)

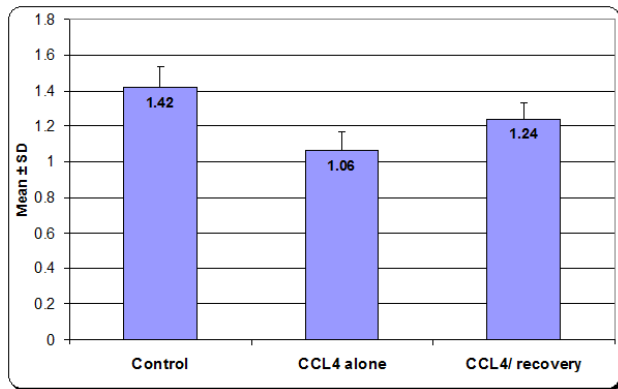
AST (U/L)	Control	CCL4 alone	CCL4/ recovery
Mean $\pm$ SD	251.00 $\pm$ 2.65	478.20 $\pm$ 2.77	385.40 $\pm$ 3.51
Range	248.0 - 255.0	474.0 - 481.0	380.0 - 389.0
<i>P-value</i> <sup>1</sup>		0.009*	0.009*
<i>P-value</i> <sup>2</sup>			0.009*



**Histogram 2:** comparing the mean values of AST level in the studied groups

**Table 3:** Mean values (± SE) of Albumin level in the studied groups (g/dl)

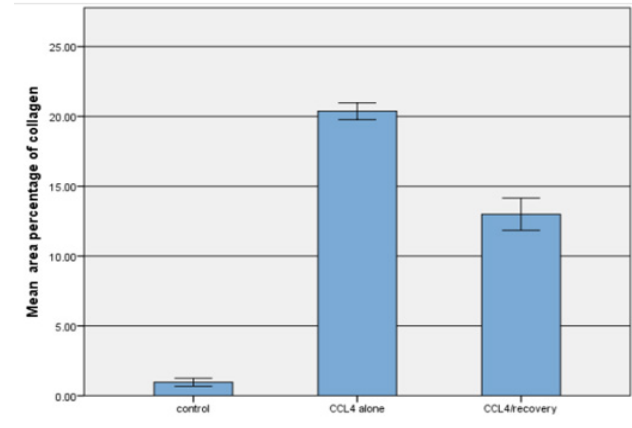
ALT (U/L)	Control	CCL4 alone	CCL4/ recovery
Mean ± SD	1.42 ± 0.11	1.06 ± 0.11	1.24 ± 0.09
Range	1.3 - 1.6	0.9 - 1.2	1.1 - 1.3
<i>P-value</i> <sup>1</sup>		0.008*	0.016*
<i>P-value</i> <sup>2</sup>			0.032*



**Histogram 3:** Comparing the mean values of Albumin level in the studied groups

**Table 4:** Mean values (±SE) of area percentage of collagen fibers in the studied groups

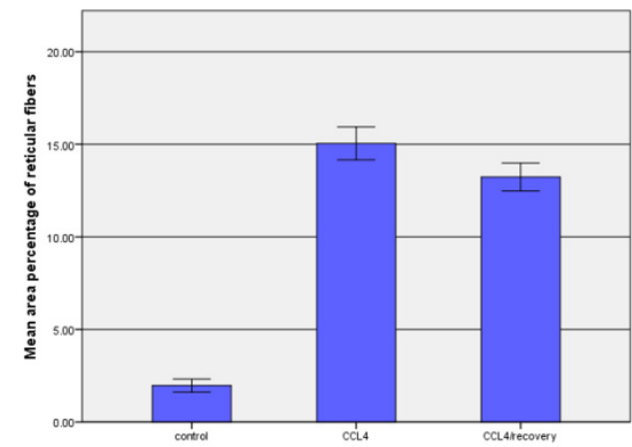
	Control	CCL4 alone	CCL4/ recovery
Mean ± SD	.96±.29	20.37 ± .59	12.99 ± 1.15
<i>P-value</i> <sup>1</sup>		0.000*	0.000*
<i>P-value</i> <sup>2</sup>			0.000*



**Histogram 4:** Comparing the mean values of area percentage of collagen fibers in the studied groups

**Table 5:** Mean values (±SE) of area percentage of reticular fibers in the studied groups

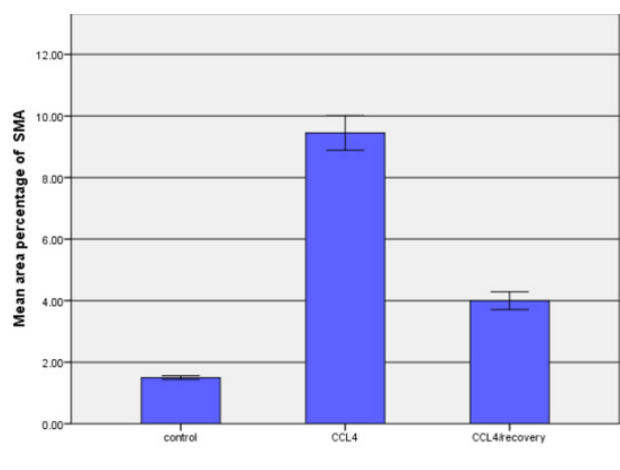
	Control	CCL4 alone	CCL4/ recovery
Mean ± SD	1.40±.057	15.05 ± .88	13.23 ± .75
<i>P-value</i> <sup>1</sup>		0.000*	0.000*
<i>P-value</i> <sup>2</sup>			0.274



**Histogram 5:** Comparing the mean values of area percentage of reticular fibers in the studied groups

**Table 6:** Mean values (±SE) of area percentage of α-SMA in the studied groups

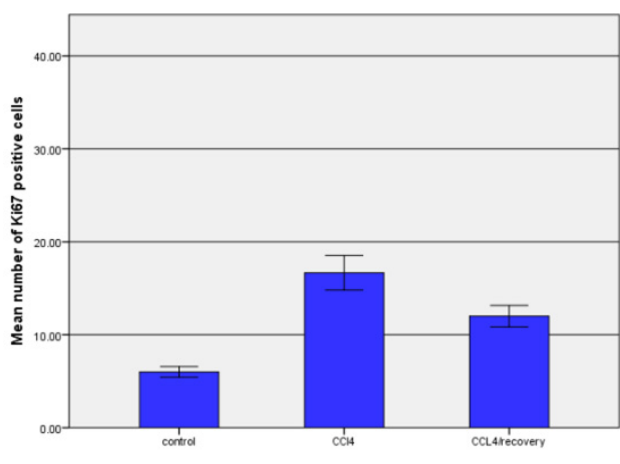
	Control	CCL4 alone	CCL4/ recovery
Mean ± SD	1.50±.05	9.45± .56	4.00 ± .28
<i>P-value</i> <sup>1</sup>		0.000*	0.003*
<i>P-value</i> <sup>2</sup>			0.000*



**Histogram 6:** Comparing the mean values of area percentage of  $\alpha$ -SMA in the studied groups

**Table 7:** Mean values ( $\pm$ SE) of number of KI67 positive cells in the studied groups

	Control	CCL4 alone	CCL4/ recovery
Mean $\pm$ SD	6.00 $\pm$ 0.57	16.66 $\pm$ 1.85	12.00 $\pm$ 1.15
<i>P</i> -value <sup>1</sup>		0.001*	0.33
<i>P</i> -value <sup>2</sup>			0.08



**Histogram 7:** Comparing the mean values of number of KI67 positive cells in the studied groups

## DISCUSSION

The liver plays a major role in maintaining the general homeostasis of the body, the general metabolism, the storage, synthesis and redistribution of nutrients<sup>[18,19]</sup>.

This study investigated the regenerative potential of the liver in mice after induction of liver fibrosis by CCL4.

In the present study, few hepatocytes expressed positive immunofluorescence for KI67 in the control group, similar observations were reported in mice<sup>[20]</sup>, using PCNA-immune staining. This finding indicated that normal hepatocytes replicated in a limited number and regulated manner<sup>[21]</sup>.

Accumulated hepatic toxins was found to induce chronic liver injury which, can leads to liver fibrosis, resulting in excessive increase in the extracellular matrix (ECM) with accumulation of collagen<sup>[22,23]</sup>.

Carbon tetrachloride (CCL4) is the most widely accepted hepatotoxin used by many researchers to study liver fibrosis in rodents. Several studies reported CCL4 model of liver fibrosis either in rats or mice. However, mice are preferred, because they exhibit a higher metabolic rate of CCL4 compared to rats<sup>[24]</sup>.

In the present study, liver tissue from CCL4 treated group revealed disturbed liver architecture, with inflammatory signs, dilated central vein surrounded with intense cellular infiltration as well as degenerative changes affecting many hepatocytes. Many cells appeared with dense nuclei and acidophilic cytoplasm. The dilated blood vessels observed in this work can be explained by portal hypertension<sup>[25]</sup>.

The intense cellular infiltration around central vein can be explained by induction of inflammation which is one of mechanisms of CCL4 induced liver toxicity<sup>[26]</sup>.

Alpha smooth muscle actin ( $\alpha$ -SMA), is a marker of Hepatic Stellate Cell activation<sup>[27]</sup>. It was detected, in this study, early then followed by collagen deposition and progressive fibrosis, leading to cirrhosis<sup>[28]</sup>.

In GII, there was a peri-sinusoidal highly positive reaction for  $\alpha$ -SMA as evidenced by increase in the area percentage of  $\alpha$ -SMA. This finding might be explained by differentiation of HSCs into myofibroblasts after liver injury. The later cells promote liver fibrogenesis<sup>[29]</sup>.

In GII, we observed significant increase in the collagen fibers around central vein and in between liver cells. Also, there was an increase in the reticular fibers content in the wall of blood vessels and in between the liver cells as evidenced by area % of collagen and reticular fibers in this study. These findings were similar to other previous studies<sup>[30]</sup>. In liver fibrosis, there is imbalance between ECM formation and degradation and there is significant increase in both collagen type I and III (reticular fibers). Activation of HSCs resulted in its conversion into proliferative myofibroblasts, that synthesize and secrete a large amount of fibers especially collagen type I and III (reticular fibers)<sup>[3]</sup>. Both types of collagen constitute the main components of the scar tissue during liver fibrosis<sup>[31]</sup>.

The degenerative effect of CCL4 on the liver can be explained by several mechanisms. One of them is oxidative stress which is a major cause. CCL4 is biotransformed into trichloromethyl free radical (CCL3), by cytochrome P-450 systems that causes lipid peroxidation and, thereby, liver damage<sup>[32]</sup>. End products of lipid peroxidation might enhance fibrosis of injured hepatocytes<sup>[33]</sup>. In the same time, necrosis as well as inflammatory response of centrilobular hepatocytes, in CCL4-treated rats, might be resulting from significant decrease in hepatic glutathione (GSH) levels<sup>[34,35]</sup>. Several cytokines after CCL4 treatment



might be also accused in activation of HSCs and finally liver fibrosis<sup>[36]</sup>.

After CCL4 treatment, a significant increase in hepatocytes positive KI67 nuclei might be due to hepatocyte regeneration which of the injured liver<sup>[37]</sup>.

Recovery of the liver after injury includes removal of dead cells and regeneration of hepatocytes to replace damaged cells. The liver is the only visceral organ that has great ability to regenerate; the hepatocytes can quickly undergo division to restore the liver architecture after injury<sup>[8]</sup>.

After injury of the liver, the hepatocytes proliferate to restore the liver mass then it stops<sup>[38]</sup>. This explains the improvement in the liver structure after CCL4 withdrawal.

In GIII, more improvement were observed but not reverted to that of control. Moderate improvement was observed in liver architecture. Moderate cellular infiltration was observed in between the liver cells compared to GII. Mild to moderate degenerative changes were observed.

Significantly high percentage of collagen as well as reticular fibers deposition was observed around central vein and in between liver cells but they were finer than group II.

Also, significant decrease in area percentage of  $\alpha$ -SMA was observed compared to group II. However, this means decrease HSC activation and stoppage of fibrosis, but recurrence is more likely to occur<sup>[39]</sup>.

KI 67 immunofluorescence showed reduced number of positive nuclei but still more than group I.

Previous studies proved that liver fibrosis is reversible in early stages before damaging the normal architecture of the liver and deteriorating the liver function<sup>[40]</sup>.

The liver is characterized by high regenerative capacity that enable it to restore its normal function within days especially after acute damage caused by hepatotoxins. However, after chronic exposure to hepatotoxins, the parenchyma not recovered from injury, and excess collagen, (glycoproteins and proteoglycans) is formed which leads to liver fibrosis<sup>[41]</sup>.

These results can be explained by that the liver cells can proliferate to replace damaged cells after CCL4 treatment, this recovery caused reduction in diseased state.

Our results are in agreement with<sup>[2,42,43,44,45]</sup> but are in contrary with<sup>[46]</sup> who found that after recovery the hepatocytes as well as liver functions were nearly similar to that of the CCL4 alone group. In addition, a progressive increase in the liver fibrosis was observed after recovery in these cases as evidenced by increased collagen fibers and  $\alpha$ -SMA positive cells.

The findings of this study demonstrated that injection of CCL4 to mice induced marked liver damage which is evidenced by significant increase in the serum levels of

AST and ALT. This is due to damage of liver cells which led to membrane permeability, and leakage of enzymes into extracellular space<sup>[47]</sup>. In liver fibrosis, there was also significantly decreased serum albumin which means liver dysfunction. These results came in agreement with those of previous studies<sup>[34,48]</sup>, who suggested that increase in the liver enzymes is an indicator of acute hepatocellular damage. In GIII of our study, there was reduction of liver enzymes but they were still higher than GI.

#### CONFLICTS OF INTEREST

There are no conflicts of interest.

#### REFERENCES

1. Lee, H. S., Li, L., Kim, H. K., Bilehal, D., Li, W., Lee, D. S., Kim, Y. H. The protective effects of Curcuma longa Linn. extract on carbon tetrachloride-induced hepatotoxicity in rats via upregulation of Nrf2. *Journal of Microbiology and Biotechnology* . (2010) 20(9): 1331-1338.
2. Aziz, M. A., Atta, H. M., Mahfouz, S., Fouad, H. H., Roshdy, N. K., Ahmed, H. H., Hasan, N. M. Therapeutic potential of bone marrow-derived mesenchymal stem cells on experimental liver fibrosis. *Clinical biochemistry*. (2007) 40(12): 893-899.
3. Friedman, S. L. Liver fibrosis—from bench to bedside. *Journal of hepatology*. (2003) 38: 38-53.
4. Guo, X. L., Liang, B., Wang, X. W., Fan, F. G., Jin, J., Lan, R., Cao, Q. Glycyrrhizic acid attenuates CCl4-induced hepatocyte apoptosis in rats via a p53-mediated pathway. *World Journal of Gastroenterology: WJG*. (2013) 19(24) 3781-3791.
5. Black, D., Bird, M. A., Samson, C. M., Lyman, S., Lange, P. A., Schrum, L. W. Behrens, K. E. Primary cirrhotic hepatocytes resist TGF $\beta$ -induced apoptosis through a ROS-dependent mechanism. *Journal of hepatology*. (2004) 40(6): 942-951.
6. Hazra, S., Xiong, S., Wang, J., Rippe, R. A., Krishna, V., Chatterjee, K., Tsukamoto. H. Peroxisome proliferator-activated receptor  $\gamma$  induces a phenotypic switch from activated to quiescent hepatic stellate cells. *Journal of Biological Chemistry* .(2004) 279 (12): 11392-11401.
7. Chang, Y. Z., Yang, L., Yang, C. Q. Migration of hepatic stellate cells in fibrotic microenvironment of diseased liver model. *Hepatobiliary Pancreat Dis Int*. (2008) 7(4): 401-405.
8. Michalopoulos, G. K., Khan, Z. Liver stem cells: experimental findings and implications for human liver disease. *Gastroenterology*. (2015) 149(4): 876-882.
9. Sakaida, I., Terai, S., Yamamoto, N., Aoyama, K., Ishikawa, T., Nishina, H., Okita, K. Transplantation of bone marrow cells reduces CCl4-induced liver fibrosis in mice. *Hepatology* (2004) 40(6): 1304-1311.

10. Bancroft, J. D., Gamble, M. (Eds.). (2008). Theory and practice of histological techniques. China: Churchill Livingstone Elsevier. 6th edition. P.725.
11. Cattoretti, G., Pileri, S., Parravicini, C., Becker, M. H., Poggi, S., Bifulco, C., Reynolds, F. Antigen unmasking on formalin-fixed, paraffin-embedded tissue sections. *The Journal of pathology* .(1993) 171(2): 83-98.
12. Shi, S. R., Guo, J., Cote, R. J., Young, L. L., Hawes, D., Shi, Y., Taylor, C. R. Sensitivity and detection efficiency of a novel two-step detection system (PowerVision) for immunohistochemistry. *Applied Immunohistochemistry & Molecular Morphology* (1999) : 7(3): 201-208.
13. Adhim, Z., Matsuoka, T., Bito, T., Shigemura, K., Lee, K. M., Kawabata, M., Shirakawa, T. In vitro and in vivo inhibitory effect of three Cox-2 inhibitors and epithelial-to-mesenchymal transition in human bladder cancer cell lines. *British journal of cancer*. (2011). 105(3), 393-402.
14. Schermer S. The blood morphology of laboratory animals. 1st ed. Philadelphia: F.A. Davies Co; 1967.
15. Reitman, S., Frankel, S. A colorimetric method for the determination of serum glutamic oxalacetic and glutamic pyruvic transaminases. *American journal of clinical pathology*. (1957). 28(1): 56-63.
16. Calvaruso, V., Burroughs, A. K., Standish, R., Manousou, P., Grillo, F., Leandro, G. & Patch, D. Computer-assisted image analysis of liver collagen: Relationship to Ishak scoring and hepatic venous pressure gradient. *Hepatology* (2009) 49(4): 1236-1244.
17. Matthews, J. N. S., Berry, G., & Armitage, P. (2002). *Statistical methods in medical research*. Blackwell Publishing company. Fourth Edition. P:277-312.
18. Diehl, A. M., Chute, J. Underlying potential: cellular and molecular determinants of adult liver repair. *The Journal of clinical investigation*.(2013) 123(5): 1858-1860.
19. Saneyasu, T., Akhtar, R., & Sakai, T. Molecular cues guiding matrix stiffness in liver fibrosis. *BioMed research international* (2016).P:1-11.
20. Gu, K., Zhao, J. D., Ren, Z. G., Ma, N. Y., Lai, S. T., Wang, J., Jiang, G. L. A natural process of cirrhosis resolution and deceleration of liver regeneration after thioacetamide withdrawal in a rat model. *Molecular biology report* (2011) s 38(3): 1687-1696.
21. Cheung, P. Y., Zhang, Q., Zhang, Y. O., Bai, G. R., Lin, M. C. M., Chan, B. Kung, H. F. Effect of WeiJia on carbon tetrachloride induced chronic liver injury. *World Journal of Gastroenterology: WJG* (2006) 12(12). 1912-1917.
22. Bataller, R., Brenner, D. A. Liver fibrosis. *The Journal of clinical investigation* (2005) 115(2): 209-218.
23. Friedman, S. L. Hepatic stellate cells: protean, multifunctional, and enigmatic cells of the liver. *Physiological reviews* (2008) 88(1): 125-172.
24. Thrall, K. D., Vucelick, M. E., Gies, R. A., Benson, J. M. Comparative metabolism of carbon tetrachloride in rats, mice, and hamsters using gas uptake and PBPK modeling. *Journal of Toxicology and Environmental Health Part A* (2000) 60(8): 531-548.
25. Hu, L. S., George, J., Wang, J. H. Current concepts on the role of nitric oxide in portal hypertension. *World Journal of Gastroenterology: WJG* (2013) 19(11). 1707-1717.
26. Bahashwan, S., Hassan, M. H., Aly, H., Ghobara, M. M., El-Beshbishy, H. A., Busati, I. Crocin mitigates carbon tetrachloride-induced liver toxicity in rats. *Journal of Taibah University Medical Sciences* (2015) 10(2): 140-149.
27. Roderfeld, M., Rath, T., Voswinckel, R., Dierkes, C., Dietrich, H., Zahner, D., Roeb, E. Bone marrow transplantation demonstrates medullar origin of CD34+ fibrocytes and ameliorates hepatic fibrosis in Abcb4<sup>-/-</sup> mice. *Hepatology* (2010). 51(1): 267-276.
28. Muhanna, N., Tair, L. A., Doron, S., Amer, J., Azzeh, M., Mahamid, M. Safadi, R. Amelioration of hepatic fibrosis by NK cell activation. *Gut* (2011) 60(1): 90-98.
29. Tacke, F., Weiskirchen, R. Update on hepatic stellate cells: pathogenic role in liver fibrosis and novel isolation techniques. *Expert review of gastroenterology & hepatology* . (2012) 6(1): 67-80.
30. Sobrevals, L., Rodriguez, C., Romero-Trevejo, J. L., Gondi, G., Monreal, I., Pañeda, A. González-Aseguinolaza, G. Insulin-like growth factor I gene transfer to cirrhotic liver induces fibrolysis and reduces fibrogenesis leading to cirrhosis reversion in rats. *Hepatology* (2010) 51(3): 912-921.
31. Liang, B., Guo, X. L., Jin, J., Ma, Y. C., Feng, Z. Q. Glycyrrhizic acid inhibits apoptosis and fibrosis in carbon-tetrachloride-induced rat liver injury. *World Journal of Gastroenterology: WJG* (2015) 21(17). 5271-5280.
32. Sisodia, S. S., Bhatnagar, M. Hepatoprotective activity of *Eugenia jambolana* Lam. in carbon tetrachloride treated rats. *Indian journal of pharmacology* (2009). 41(1). 23-27.
33. Fu, Y., Zheng, S., Lin, J., Ryerse, J., Chen, A. Curcumin protects the rat liver from CCl4-caused injury and fibrogenesis by attenuating oxidative stress and suppressing inflammation. *Molecular pharmacology* (2008) . 73(2): 399-409.
34. Zhen, M. C., Wang, Q., Huang, X. H., Cao, L. Q., Chen, X. L., Sun, K., Zhang, L. J. Green tea polyphenol epigallocatechin-3-gallate inhibits oxidative damage

- and preventive effects on carbon tetrachloride-induced hepatic fibrosis. *The Journal of nutritional biochemistry* (2007) 18(12): 795-805.
35. Heindryckx, F., Colle, I., Van Vlierberghe, H. Experimental mouse models for hepatocellular carcinoma research. *International journal of experimental pathology* (2009) 90(4): 367-386.
  36. Iwaisako, K., Jiang, C., Zhang, M., Cong, M., Moore-Morris, T. J., Park, T. J., Meng, F. Origin of myofibroblasts in the fibrotic liver in mice. *Proceedings of the National Academy of Sciences* (2014) 111(32):E3297-E3305.
  37. Wiemann, S. U., Satyanarayana, A., Tshuridu, M., Tillmann, H. L., Zender, L., Klempnauer, J., Rudolph, K. L. Hepatocyte telomere shortening and senescence are general markers of human liver cirrhosis. *The FASEB journal* (2002). 16(9):935-942.
  38. Fausto, N. Liver regeneration. *Journal of hepatology* (2000) 32, 19-31.
  39. Troeger, J. S., Mederacke, I., Gwak, G. Y., Dapito, D. H., Mu, X., Hsu, C. C., Schwabe, R. F. Deactivation of hepatic stellate cells during liver fibrosis resolution in mice. *Gastroenterology* (2012) 143(4): 1073-1083.
  40. Lin, X., Bai, F., Nie, J., Lu, S., Lu, C., Zhu, X., Huang, Q. Didymin alleviates hepatic fibrosis through inhibiting ERK and PI3K/Akt pathways via regulation of Raf kinase inhibitor protein. *Cellular Physiology and Biochemistry* (2016) 40(6):1422-1432.
  41. Seifert, W. F., Roholl, P. J., Blauw, B., Van der Ham, F., van Thiel-De Ruyter, C. F., Seifert-Bock, I., Brouwer, A. Fat-storing cells and myofibroblasts are involved in the initial phase of carbon tetrachloride-induced hepatic fibrosis in BN/BiRij rats. *International journal of experimental pathology* (1994) 75(2). 131-146.
  42. Park, J. A., Cha, J. H., Choi, E. S., Yoon, S. K., Bae, S. H. Therapeutic potential of human mesenchymal stem cells derived from amnion and bone marrow in a rat model of acute liver injury and fibrosis. *Tissue engineering and Regenerative medicine*, (2011). vol. 8, No. 4, pp: 422-431.
  43. Pan, X. N., Zheng, L. Q., Lai, X. H. Bone marrow-derived mesenchymal stem cell therapy for decompensated liver cirrhosis: a meta-analysis. *World Journal of Gastroenterology: WJG* (2014) 20(38).14051-14057.
  44. Song, Y. M., Lian, C. H., Wu, C. S., Ji, A. F., Xiang, J. J., Wang, X. Y. Effects of bone marrow derived mesenchymal stem cells transplanted via the portal vein or tail vein on liver injury in rats with liver cirrhosis. *Experimental and therapeutic medicine* (2015) 9 (4): 1292-1298.
  45. Truong, N. H., Nguyen, N. H., Le, T. V., Vu, N. B., Huynh, N., Nguyen, T. V., Pham, P. V. Comparison of the treatment efficiency of bone marrow-derived mesenchymal stem cell transplantation via tail and portal veins in CCl4-induced mouse liver fibrosis. *Stem cells international*, (2016).p:1-13.
  46. Ahmed, S. K., Mohammed, S. A., Khalaf, G., Fikry, H. Role of bone marrow mesenchymal stem cells in the treatment of CCL4 induced liver fibrosis in albino rats: a histological and immunohistochemical study. *International journal of stem cells* (2014). 7(2). 87-97.
  47. Vuda, M., D'Souza, R., Upadhya, S., Kumar, V., Rao, N., Kumar, V., Mungli, P. Hepatoprotective and antioxidant activity of aqueous extract of *Hybanthus enneaspermus* against CCl4-induced liver injury in rats. *Experimental and toxicologic pathology* (2012). 64(7-8): 855-859.
  48. Elhalwagy, M. E., Darwish, N. S., Zaher, E. M. (Prophylactic effect of green tea polyphenols against liver and kidney injury induced by fenitrothion insecticide. *Pesticide biochemistry and physiology* 2008).91(2): 81-89.

## الملخص العربي

## هل يمكن للكبد تجديد القدرة على استعادة بنيته الطبيعية في التليف المستحث برابع كلوريد الكربون في الفئران؟ دراسة هستولوجية وهستوكيميائية مناعية

هبة محمد سعد الدين<sup>١،٢</sup>، نشوى أحمد محمد مصطفى<sup>٢</sup>، رندا عبدالعزيز محمد<sup>٢</sup>  
<sup>١</sup>قسم علم الأنسجة وبيولوجيا الخلية، كلية الطب، جامعة الجوف، المملكة العربية السعودية  
<sup>٢</sup>قسم علم الأنسجة وبيولوجيا الخلية، كلية الطب - جامعة أسيوط، مصر

**الخلفية:** تليف الكبد هو مشكلة صحية كبيرة في مصر وتهديد خطير لصحة الإنسان. ويتميز بتكرار الإصابة لأنسجة الكبد مما يؤدي إلى التراكم المفرط لمادة النسيج خارج الخلية. الكبد هو العضو الحشوي الوحيد الذي يمتلك قدرة فريدة على التجدد.

**الهدف من البحث:** لمعرفة دور القدرة التجديدية للكبد لاستعادة البنية الطبيعية بعد سحب رابع كلوريد الكربون (CCL4) في الفئران.

**المواد والطرق:** تم استخدام عدد ثلاثين من الفئران الذكور في هذه الدراسة. تم تقسيم الحيوانات عشوائياً إلى ثلاثة مجموعات (١٠ فئران لكل منهما): المجموعة ١: (مجموعة التحكم = GI). المجموعة الثانية (مجموعة رابع كلوريد الكربون). تمت حقن الفئران باستخدام ١ مل / كجم رابع كلوريد الكربون (CCL4) الذائبة في زيت الزيتون (١ : ١) مرتين في الأسبوع لمدة أربعة أسابيع داخل الغشاء البريتوني. ثم في نهاية الأسبوع الرابع تم التضحية بهم. المجموعة الثالثة (CCL4 / مجموعة الاستعادة = GIII): تم حقنها برابع كلوريد الكربون CCL4 كالمجموعة السابقة ، ثم تركت لمدة أربعة أسابيع أخرى دون أي تدخل قبل التضحية. في نهاية التجربة ، تم تشريح الكبد فوراً ومعالجته من أجل الفحص النسيجي والمناعي الكيميائي.

**النتائج:** في المجموعة الثانية ، كان هناك خلل ملحوظ في بنية الكبد في شكل ارتشاح خلوي ملحوظ مع فجوات خلوية مع زيادة كبيرة في الكولاجين والألياف الشبكية ، وزيادة في الصبغة الكيميائية المناعية لاكتين العضلات الملساء في الخلايا النجمية الكبدية. وكان هناك زيادة في تكاثر خلايا الكبد كما هو مبين من خلال زيادة الصبغة المناعية الفلوريسينية ل KI67. في المجموعة الثالثة ، لوحظ تحسن معتدل في بنية الكبد. كما لوحظ انخفاض كبير في انزيمات الكبد ذو دلالة احصائية . من ناحية أخرى ، ازداد بشكل ملحوظ مستوى الزلال في مصل الدم بالمقارنة بالمجموعة الثانية.

**الخلاصة:** نتج عن انسحاب CCL4 تحسن معتدل في بنية الكبد. و لكن التعرض المزمن له فاق القدرة التجديدية للكبد لاستعادة بنيته الطبيعية.